AD-A069 461 NAVAL RESEARCH LAB WASHINGTON DC F/G 20/5
THE NON-LINEAR THEORY OF EFFICIENCY ENHANCEMENT IN THE ELECTRON--ETC(U)
APR 79 P SPRANGLE, R A SMITH
UNCLASSIFIED NRL-MR-3983 NL

| OF |
AD
A069461

END
DATE
FILMED
7-79
DDC

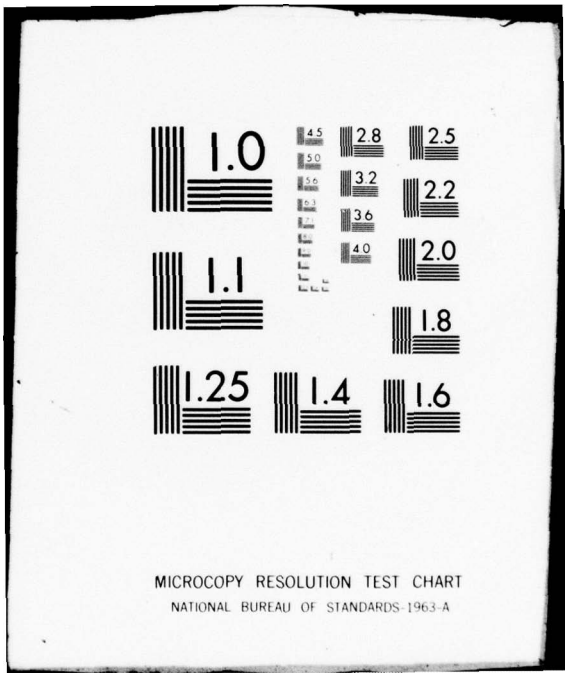
1.0
1.1
1.25
1.4
1.6
1.8
2.0
2.2
2.5
2.8
3.2
3.6
4.0
4.5
5.0
5.6
6.3
MICROCOPY RESOLUTION TEST CHART
NATIONAL BUREAU OF STANDARDS-1963-A

(12) LEVEL II Sub3

NRL Memorandum Report 3983

The Non-Linear Theory of Efficiency Enhancement in the Electron Cyclotron Maser

P. SPRANGLE

Plasma Physics Division

and

ROBERT A. SMITH

Jaycor
Alexandria, VA 22304

April 18, 1979

NAVAL RESEARCH LABORATORY
Washington, D.C.

SECURITY CLASSIFICATION OF THIS PAGE (When Data Entered)

REPORT DOCUMENTATION PAGE

READ INSTRUCTIONS BEFORE COMPLETING FORM

1. REPORT NUMBER: NRL Memorandum Report 3983
2. GOVT ACCESSION NO.
3. RECIPIENT'S CATALOG NUMBER

4. TITLE (and Subtitle): THE NON-LINEAR THEORY OF EFFICIENCY ENHANCEMENT IN THE ELECTRON CYCLOTRON MASER.
5. TYPE OF REPORT & PERIOD COVERED: Interim report on a continuing NRL problem.
6. PERFORMING ORG. REPORT NUMBER

7. AUTHOR(s): P. Sprangle and R. A. Smith
8. CONTRACT OR GRANT NUMBER(s)

9. PERFORMING ORGANIZATION NAME AND ADDRESS: Naval Research Laboratory, Washington, D.C. 20375
10. PROGRAM ELEMENT, PROJECT, TASK AREA & WORK UNIT NUMBERS: NRL Problem R18-12; DOE EX77A341015;†

11. CONTROLLING OFFICE NAME AND ADDRESS
12. REPORT DATE: April 18, 1979
13. NUMBER OF PAGES: 26

14. MONITORING AGENCY NAME & ADDRESS(if different from Controlling Office)
15. SECURITY CLASS. (of this report): Unclassified
15a. DECLASSIFICATION/DOWNGRADING SCHEDULE

16. DISTRIBUTION STATEMENT (of this Report): NRL-MR-3983

Approved for public release; distribution unlimited.

17. DISTRIBUTION STATEMENT (of the abstract entered in Block 20, if different from Report): F54581

18. SUPPLEMENTARY NOTES

*Jaycor, Alexandria, Va. 22304

† R08-92-NAVELEX-WR89110-XF54581007; R08-95-BMDATC-W31RPD-83-2107

19. KEY WORDS (Continue on reverse side if necessary and identify by block number)

Non-Linear Particle Dynamics
Electron Cyclotron Maser
Efficiency Enhancement

20. ABSTRACT (Continue on reverse side if necessary and identify by block number)

We present a nonlinear analysis of the single particle dynamics in an electron cyclotron maser oscillator and show that the efficiency can be dramatically enhanced by appropriately contouring the system parameters. The beam electrons can be prebunched in phase to form a macro-particle in phase space such that beam kinetic energy is not extracted. After forming a phase bunched electron beam, either the applied magnetic field or the cavity electromagnetic field can be spatially varied in such a way as to extract virtually all the electron transverse kinetic energy. Without such contouring,

next page

(Continued)

DD FORM 1 JAN 73 1473 EDITION OF 1 NOV 65 IS OBSOLETE
S/N 0102-014-6601

251 950

20. Abstract (Continued)

the transverse efficiency is typically ≤ 40%. An example is presented in which the transverse efficiency is increased from 36% (in uniform fields) to 75% by increasing the applied magnetic field by ~ 6%. The present analysis can readily be extended to the case of a maser amplifier.

CONTENTS

THE NON-LINEAR THEORY OF EFFICIENCY ENHANCEMENT IN THE ELECTRON CYCLOTRON MASER

I. INTRODUCTION

Radiation sources based on the electron cyclotron maser mechanism are perhaps the most efficient devices for generating high continuous power in the millimeter and submillimeter regimes. The first theoretical work[1-3] on the cyclotron maser mechanism showed the relativistic nature of the instability while experimental confirmation came shortly afterwards.[4,5] Since this early work, theoretical and experimental[21-27] research on the maser amplifier and oscillator has indicated that these devices could have great practical values in areas ranging from RF heating of fusion plasmas to new radar systems. For applications such as plasma heating, high efficiency is of prime importance.

The operation of the electron cyclotron maser oscillator can be viewed qualitatively as the exchange of energy from a system of nonlinear oscillators (electrons) to the fields of a cavity. We describe briefly the steady state operation of a maser cavity in which electrons are entering and radiation is emitted at a uniform rate. The electrons enter the cavity, gyrating about an applied longitudinal magnetic field. Since the electron cyclotron frequency is energy dependent, because of relativistic effects, these electrons can be viewed as nonlinear (or nonisochronous) oscillators. The electron cyclotron frequency decreases as the electron kinetic energy increases. We choose the initial conditions to be such that the cyclotron frequency of the entering electrons is slightly lower than the fixed Doppler shifted frequency of the cavity field. As the initially randomly phased electrons drift through the cavity some of them lose, while others will

Manuscript submitted February 26, 1979.

gain, kinetic energy, depending on the initial value of their Larmor phase with respect to the electric field. The electrons which gain energy undergo a decrease in rotational frequency, causing them to move further from resonance with the cavity fields. Those electrons which lose kinetic energy, on the other hand, get closer to resonance with the fields and lose energy faster and for a longer time. Thus it is possible to have a net decrease in electron kinetic energy for a time after the electrons enter the cavity. If the electrons were to remain within the cavity they would eventually begin to gain back a portion of the net kinetic energy lost. However, in designing a practical cavity, the transit time of the electrons is made equal to the time it takes the average electron kinetic energy to reach a minimum. In the steady state the Q of the cavity is chosen such that the radiated power just balances the rate of kinetic energy lost by the electrons. For a comprehensive treatment of the nonlinear and linear theory of the cyclotron maser amplifier see Ref. (17). A number of excellent review papers[8,28–30] are available which discuss the physical mechanism and applications of the maser in more detail.

Theoretical and experimental progress has been made in improving the maser oscillator efficiency by contouring the walls and thus the fields of the cavity. Experimental efficiencies of $\sim$40% at wavelengths of $\sim$9 mm and continuous powers of $\sim$20 kW have been achieved.[21]

It is the purpose of this paper to analyze the nonlinear particle dynamics in the cyclotron maser and address the problem of efficiency enhancement. We show that by appropriately contouring the applied magnetic field or the cavity electric field as a function of axial position, the beam electrons can be prebunched in phase, resulting in a significant increase in efficiency over the already high intrinsic value. Although we analyze a maser oscillator configuration, our method of enhancing the efficiency is applicable to a maser amplifier with minor changes.

II. ANALYSIS

a. Maser Cavity Model

We shall consider a steady state maser cavity oscillator with the geometry shown in Fig. 1. The electron beam drifts in the z-direction and gyrates about the applied axial magnetic field $B_0\hat{e}_z$. The beam consists of a thin current sheet, uniform in the y-direction, with the guiding centers of the electrons initially uniformly distributed on the $x = 0$ plane. For a sufficiently low-current beam, we may take the cavity fields to be given by the unperturbed normal modes of the cavity. For definiteness we assume that the beam drives a single $TE_{0,m,n}$ mode. The only non-vanishing field components for this mode are

$$E_y(x, z, t) = \sum_{m,n} E_{m,n} \cos(\omega_{m,n} t + \phi_{m,n}) \sin(K_n z) \sin(k_m (a - x))$$

$$B_x(x, z, t) = \sum_{m,n} \frac{cK_n}{\omega_{m,n}} E_{m,n} \sin(\omega_{m,n} t + \phi_{m,n}) \cos(K_n z) \sin(k_m (a - x)),$$

$$B_z(x, z, t) = \sum_{m,n} \frac{ck_m}{\omega_{m,n}} E_{m,n} \sin(\omega_{m,n} t + \phi_{m,n}) \sin(K_n z) \cos(k_m (a - x)), \qquad \text{(1a,b,c)}$$

where $E_{m,n}$ and $\phi_{m,n}$ is the mode amplitude and phase, $k_m = m\pi/2a$, $K_n = n\pi/L$, $\omega_{m,n} = c\sqrt{k_m^2 + K_n^2}$ and $m,n = 1, 2, 3, \ldots$. For strong coupling, the electric field must be maximum at the beam location, i.e, m odd, and have a frequency close to the electron cyclotron frequency.

b. Particle Dynamics

The particles enter the cavity at $z = 0$, randomly phased, with the same axial velocity $v_{oz} = \beta_{oz} c$ and the same transverse velocity $v_{o\perp} = \beta_{o\perp} c$. In order to obtain tractable nonlinear orbit equations we make a number of simplifying assumptions, all of which are physically well founded. We assume that the transverse wavelength of the cavity mode, $2\pi/k_m$, is large compared to the electron Larmor radius as well as the excursions of the particle guiding centers in

the x-direction, hence $|k_m x| << 1$, $\sin(k_m(a - x)) \approx \sin(k_m a)$ and $\cos(k_m(a - x)) \approx x k_m \sin(k_m a)$ for m odd. The particle velocities are considered to be mildly relativistic, *i.e.*, $(\dot{z}/c)^2$, $(\dot{x}/c)^2$ and $(\dot{y}/c)^2 << 1$. Finally we assume that the cavity is long, *i.e.*, $L >> 2a$, and that the cavity field amplitude is small compared to the applied magnetic field, *i.e.*, $|E_{m,n}/B_0| << 1$.

For a single *TE* cavity mode the orbit equations, in the absence of self-fields, take the approximate form

$$\frac{d}{dt}(\gamma\dot{x}) \approx -\Omega_0 \dot{y}$$

$$\frac{d}{dt}(\gamma\dot{y}) \approx \Omega_0 \dot{x} - \frac{|e|}{m_0} E \sin(ka)\sin(Kz)\cos(\omega t + \phi)$$

$$\frac{d(\gamma\dot{z})}{dt} \approx 0 \qquad \text{(2a,b,c)}$$

where $\gamma = (1 - (\dot{x}^2 + \dot{y}^2 + \dot{z}^2)/c^2)^{-1/2} \geq 1$, $\Omega_0 = |e|B_0/m_0 c$. The subscripts on $E_{m,n}$, k_m, K_n, $\omega_{m,n}$ and $\phi_{m,n}$ have been dropped. In obtaining Eqs. (2), some higher order terms have been neglected, these terms are typically smaller than the dominant terms by the factor $(\dot{z}/c)(cK/\omega)(xk) << 1$.

From Eqs. (2a) and (2c) we find that the canonical momenta in the x direction as well as the axial velocity of the particles in the cavity are approximately conserved, *i.e.*, $\gamma\dot{x} + \Omega_0 y = 0$ and $\dot{z} = v_{0z}$. Making use of these two approximate constants, Eq. (2b) can be put into the form

$$\ddot{y} + \Omega_0^2(1 - \beta_{0z}^2 - \Omega_0^2 y^2/c^2 - \dot{y}^2/c^2)y$$

$$= -\frac{|e|}{m_0} E \sin(ka)\sin(K v_{0z}(t - t_0))\cos(\omega t + \phi), \qquad (3)$$

where t_0 is the entry time of the particle into the cavity and we have used the approximation $\gamma \approx 1 + (\beta_{0z}^2 + \Omega_0^2 y^2/c^2 + \dot{y}^2/c^2)/2$. The phase bunching process in the cyclotron maser

occurs on a time scale which is slow compared to the cavity wave period or electron cyclotron period. Since $K v_{oz} << \omega \approx \Omega_o$ we see that the solution to Eq. (3) can be written in the form

$$y = r(t)\sin(\omega t + \theta(t)) \tag{4}$$

where r and θ vary slowly in time, *i.e.*, $|\dot{r}/r|, \dot{\theta} << \omega$. Substituting Eq. (4) into (3) and using the approximations $\Omega_o^2 y^2 + \dot{y}^2 \approx \omega^2 y^2$ and

$$\Omega_o^2(1 - \beta_{oz}^2 - \omega^2 r^2/c^2) - \omega^2 \approx -2\omega\{\omega - \Omega_o[1 - (\beta_{oz}^2 + \omega^2 r^2/c^2)/2]\},$$

we find that r and θ satisfy the following equations:

$$\dot{r} = -\epsilon c \sin(K v_{oz} t)\cos(\theta - \phi),$$

$$\dot{\theta} = \Omega_o/\gamma(r) - \omega + \frac{\epsilon c}{r}\sin(K v_{oz} t)\sin(\theta - \phi), \tag{5a,b}$$

where $\gamma(r) = 1 + 1/2(\beta_{oz}^2 + \omega^2 r^2/c^2) \gtrsim 1$ and $\epsilon \equiv (E/2B_0)\sin(ka) << 1$. In deriving Eqs. (5) we have neglected small terms in $\ddot{r}$, $\ddot{\theta}$, $\dot{r}\dot{\theta}$ and $\dot{\theta}^2$. Note that the particle time of entry, t_o, can be arbitrarily set equal to zero without loss of generality.

Since $\Omega_o \approx \omega$, the term $\omega r/c$ can be identified as the magnitude of the transverse particle velocity. The kinetic energy of a particle in the cavity is $E = (\gamma - 1)m_o c^2$ and is a function of r only. The evolution of r, given by the simultaneous solutions of Eqs. (5), gives the particle energy as a function of time (axial position) in the cavity. The nonisochronous nature of the maser process is evidenced by the fact that the electron cyclotron frequency (the first term on the RHS of Eq. (5b)) is energy dependent because of the relativistic term $\omega^2 r^2/c^2$. The energy dependent cyclotron frequency is responsible for the phase bunching of the particle ensemble, which is initially distributed randomly in θ.

c. Forward or Backward Wave Coupling

The standing wave associated with a cavity mode is the superposition of a forward and a backward propagating wave. We may further simplify the description of the nonlinear particle

dynamics contained in Eqs. (5) by noting that under certain conditions the beam particles will predominantly couple to either the forward or backward wave. This will permit us to derive a useful constant of the motion for analyzing the nonlinear dynamics of the particles. To see this we define the variable $\xi_\pm = \theta \pm K v_{oz} t$ and note that for small cavity field levels, *i.e.*, $\epsilon \to 0$, $\xi_\pm$ is appropiately given by

$$\xi_\pm \approx \Delta\omega_\pm \, t + \theta_o$$

where $\Delta\omega_\pm = \omega - \Omega_o/\gamma(r_o) \mp K v_{oz}$. Interaction with the forward wave implies $|\Delta\omega_-| >> |\Delta\omega_+| \approx 0$ while for the backward wave resonance we would have $|\Delta\omega_+| >> |\Delta\omega_-| \approx 0$. If, however, $|\Delta\omega_+| \approx |\Delta\omega_-|$, both waves couple to the beam about equally and the overall interaction is weak, resulting in low efficiency. It is, therefore, desirable and possible, by properly choosing the system parameters, to have one of the wave interactions dominate over the other. If this is done the nonlinear coupled equations in (5a,b) can be put into the form

$$\dot{r} = \mp \frac{\epsilon c}{2} \cos \xi_\pm$$

$$\dot{\xi}_\pm = \Omega_o/\gamma(r) - \omega \pm K v_{oz} \pm \frac{\epsilon c}{2r} \sin \xi_\pm \qquad (6a,b)$$

where without loss of generality, ϕ has been set equal to $3\pi/2$ in Eqs. (6) and the upper (lower) sign corresponds to forward (backward) wave resonance. These equations are identical in form to those describing the particle orbits in a cavity field that is uniform in z. For definiteness we will consider only the forward wave resonance case (upper sign); this implies that $\omega > \Omega_o/\gamma$. With obvious changes in parameter definitions our results apply directly to the backward wave resonance case. Dropping the subscript on ξ_+ we get

$$\dot{r} = \frac{-\epsilon c}{2} \cos \xi,$$

$$\dot{\xi} = \Omega_o/\gamma(r) - \tilde{\omega} + \frac{\epsilon c}{2r} \sin \xi, \qquad (7a,b)$$

where $\tilde{\omega} = \omega - K v_{oz}$. This system of equations is equivalent to that obtained from the well known Duffing equation on a slow time scale.[11] The nonlinear orbits defined by Eqs. (7) can be shown to have the following constant of motion

$$C(r,\xi) = \frac{1}{\Omega_o \omega}(\tilde{\omega} - \Omega_o/\gamma(r))^2 - \epsilon \frac{\omega r}{c} \sin \xi \tag{8}$$

Typical curves in (r,ξ) space are shown in Fig. (2) for various values of C. In general, particles may lie on open or closed (trapped) orbits.

Particles starting on a particular constant-of-motion curve remain on this curve. The rate at which the particles move along the C-curves is governed by the solutions of the orbit equations in (7). We assume no interaction among the particles themselves (*i.e.*, we neglect space-charge effects). Thus we may represent the beam by an ensemble of a small number of particles, typically 32. Numerically solving Eqs. (7), for such an initial ensemble of particles, the distribution of particles for various times (or axial positions within the cavity) is shown in Fig. (3). The particles enter the cavity uniformly distributed in ξ over an interval of 2π radians, all with the same initial value of transverse velocity, *i.e.*, $r = r_o$, see Fig. (3a). As time progresses, the particles move along their respective C-curves. In the linear regime (Fig. 3b) a significant amount of spreading in r along with a small degree of bunching in ξ has developed. As the particles begin to bunch in phase angle ξ (Fig. 3c) most of them are contained within the energy loss regime $-\pi/2 < \xi < \pi/2$ and considerable spreading in r has occurred. The particles are distributed over a wide range of C-curves, with two ensuing consequences. First, as the particles lose energy they move out of the energy loss region, $-\pi/2 < \xi < \pi/2$. Secondly not all the particles reach their minimum energy at the same time. Figure (3d) shows the particle ensemble in the saturated state where the particles are deeply trapped and the average

transverse kinetic energy is at a minimum. If permitted, the particle ensemble would continue to rotate and regain the lost kinetic energy.

The efficiency of energy extraction from the particles is defined as

$$\eta(t) = N_p^{-1} \sum_{i=1}^{N_p} (\gamma(r_i(t)) - \gamma(r_o))/(\gamma(r_o) - 1) \tag{9}$$

where

$$\gamma(r_i(t)) = \gamma(r_o) + \omega^2 c^{-2}(r_i^2(t) - r_o^2)/2$$

(c.f. below Eqs. (5)), $r_o = r_i(t=0)$ and $r_i(t)$ is the Larmor radius of the ith particle which entered the cavity with phase angle $0 < \xi_i < 2\pi$, and N_p is the number of particles in the ensemble. In order to have a standard comparison between various sets of parameters we shall henceforth consider the transverse efficiency, defined by $\eta_\perp(t) = \eta(t)(\gamma(r_o) - 1)/(\omega r_o/c)^2$. Thus, $\eta_\perp(t)$ is the efficiency associated with the transverse beam kinetic energy and is independent of v_{oz}. The transverse energy efficiency is given in Fig. (4) as a function of time for the parameters of Fig. (3). The net energy extracted reaches a maximum at $t = t_s = 165/\tilde{\omega}$; the length of the actual cavity would be $L = v_{oz} t_s$. Figure (5) shows the peak transverse efficiency as a function of $\tilde{\epsilon}$, for $v_{o\perp}/c = 0.3$ and various values of the frequency mismatch parameter $\Delta\omega = \tilde{\omega} - \Omega_o/\gamma(r_o)$. From these curves we see that the maximum transverse efficiency is approximately 40%. This maximum intrinsic efficiency of approximately 40% is characteristic for the range of $v_{o\perp}/c$ of interest in the maser. We note that in our treatment the steady state value of ϵ is taken to be compatible with the Q of the cavity.

III. ENHANCEMENT OF MASER EFFICIENCY

A qualitative appreciation of the nonlinear particle dynamics can be gained from an examination of the C-curves and phase space trajectories, depicted in Figs. 2 and 3. We note that

since the particles are not all on the same C-curves they reach their minimum energies at different times. Furthermore the minimum energy varies widely over the ensemble of particles. We are thus led to the conclusion that the efficiency can be dramatically increased by first prebunching the particles in phase space. The resulting "macro-particle" can then be placed on a set of C-curves for which virtually 100% of the transverse kinetic energy is extracted.

To see in detail how this can be accomplished we must examine the basic orbit equations in (7). We consider the linear regime of these equations by expanding r and ξ in powers of the normalized electric field ϵ. For ϵ sufficiently small we can write $r \approx r^{(0)} + \epsilon r^{(1)}$ and $\xi \approx \xi^{(0)} + \epsilon\xi^{(1)}$ where $r^{(0)}$, $r^{(1)}$, $\xi^{(0)}$, $\xi^{(1)}$ are independent of ϵ. The solution of (7) in the linear regime is $r^{(0)} = r_0$, $\xi^{(0)} = \xi_0 - \Delta\omega t$ and

$$r^{(1)} = \frac{c}{2\Delta\omega}\,(\sin(\xi_0 - \Delta\omega t) - \sin\xi_0)\,,$$

$$\xi^{(1)} = \frac{c}{2\Delta\omega r_0}\left[\left(1 - \frac{\Omega_0}{\Delta\omega}\,\frac{\omega^2 r_0^2}{c^2}\right)(\cos(\xi_0 - \Delta\omega t) - \cos\xi_0) + \Omega_0 t\,\frac{\omega^2 r_0^2}{c^2}\sin\xi_0\right] \quad (10a,b)$$

where $|\epsilon r^{(1)}| \ll r^{(0)}$, and $|\epsilon\xi^{(1)}| \ll \xi^{(0)}$. The standard deviations of r and ξ are measures of the spreads of the particle ensemble in phase space and are defined respectively as $\sigma_r = (\langle r^2\rangle - \langle r\rangle^2)^{1/2}$ and $\sigma_\xi = (\langle\xi^2\rangle - \langle\xi\rangle^2)^{1/2}$ where $\langle(\ldots)\rangle = (2\pi)^{-1}\int_0^{2\pi} d\xi_0(\ldots)$. In the linear regime we find

$$\sigma_r = \alpha(1 - \cos\Delta\omega t)^{1/2} r_0,$$

$$\sigma_\xi = \left\{\frac{\pi^2}{3} - 2\alpha\left[\frac{\omega^2 r_0^2}{c^2}\,\Omega_0 t + \left(1 - \frac{\Omega_0}{\Delta\omega}\,\frac{\omega^2 r_0^2}{c^2}\right)\sin\Delta\omega t\right]\right\}^{1/2}, \quad (11a,b)$$

where $\alpha = \epsilon c/(2r_0\Delta\omega)$ will be denoted as the "bunching parameter." The mean values of r and ξ are $\langle r\rangle = r_0$ and $\langle\xi\rangle = \pi - \Delta\omega t$. These linearized equations are valid if $\alpha \ll 1$. From Eqs. (11) we note that σ_r is bounded while σ_ξ decreases secularly in time. Therefore, if $\alpha \ll 1$, the particle distribution will bunch into a macro-particle with phase space dimensions of

$$\Delta r \approx \sqrt{2}\alpha r_0,$$

$$\Delta\xi \approx (\pi^2/3 - 2\alpha(\omega r_0/c)^2\Omega_0 t)^{1/2}, \qquad (12a,b)$$

Note that the expression for $\Delta\xi$ is invalid for times such that $\Omega_0 t \gtrsim \pi^2(6\alpha(\omega r_0/c)^2)^{-1}$. The point to be made by Eqs. (12) is that Δr is bounded and $\Delta\xi$ initially decreases with time if α is sufficiently small. The formation and dimensions of the macro-particle in phase space is schematically depicted in Fig. 6. As shown in Fig. 6, all the particles lie on open trajectories and the formation of the macro-particle takes place over many cyclotron periods, with only a small degree of spreading in r.

We can tailor the bunching parameter such as to achieve minimum σ_ξ when the macro-particle enters the energy loss region $\cos\xi > 0$. When the macro-particle enters this region the bunching parameter can be increased such as to deform the trajectories of the macro-particle onto a bundle of closed C-curves for which virtually all the transverse kinetic energy can be extracted. The change in α should occur over an axial distance roughly equal to $v_{0z}/\Delta\omega$, in order to ensure that the macro particle remains in the energy loss region. The bunching parameter can be changed as a function of axial position in the cavity by (i) varying K as a function of z (for example by axially contouring the cavity wall radius) and/or (ii) varying the external magnetic field, B_0, as a function of z. From the definition of the bunching parameter, $\alpha = \epsilon c/(2r_0\Delta\omega)$, we see that these methods can lead to a large fractional change in α with only modest changes in either K or B_0. As an illustration of contouring α by method (ii) we choose the magnetic field variation depicted in Fig. 7. The initial parameters are $\epsilon = 0.004$, $\beta_{0\perp} = 0.3$ and $\Delta\omega/\tilde{\omega} = 0.08$. The intial value of the bunching parameter is $\alpha = 0.077$ (see Fig. 7). The particles reach their maximum degree of bunching at $\tilde{\omega}t \approx 225$, just before entering the energy loss region, see Fig. 8. At this point the frequency mismatch is decreased gradually to the value $\Delta\omega/\tilde{\omega} = 0.02$ at $\tilde{\omega}t = 260$. This is accomplished by increasing the external magnetic field

by about 6%. The bunching parameter has the final value $\alpha = 0.31$ at the end of the transition region and the macro particle is now on a trapped orbit. The maximum transverse kinetic energy loss occurs at $\tilde{\omega}t = 400$ resulting in a transverse efficiency of $\eta_\perp = 75\%$. The transverse efficiency as a function of time is shown in Fig. 9. As shown in Fig. 5, without contouring the applied magnetic field the transverse efficiency is 36% for these parameters with constant $\Delta\omega/\tilde{\omega} = 0.02$.

IV. CONCLUSION

We have shown that dramatic increases in the efficiency of the maser oscillator can be achieved by appropriately tailoring either the applied axial magnetic or the cavity field (cavity wall radius). It should be noted that this approach can be directly applied, with appropriate modifications, to a maser amplifier device. We have illustrated in detail an example for which the applied magnetic field is tailored. The requisite field variations are quite modest and technologically straightforward. No attempt has been made to obtain an optimum field profile, as it is our purpose to present the general principle of efficiency enhancement and show that dramatic increases can be readily achieved. As a standard of comparison we have considered only the transverse efficiency, $\eta_\perp$, which is independent of v_{0z}. In principle, the energy associated with the longitudinal motion may be largely recovered by using depressed collectors, so that the overall system efficiency may be made to approach $\eta_\perp$.

ACKNOWLDGEMENTS

We thank Drs. K. R. Chu, V. L. Granatstein and A. T. Drobot for stimulating discussions.

REFERENCES

1. R.Q. Twiss, Australian J. Phys. 11, 564 (1958).

2. J. Schneider, Phys Rev. Lett. 2, 504 (1959).

3. A.V. Gaponov, Izv. Vyssh, Uchebn, Zaved., Radiofizi, 2, 450 (2959).

4. R.H. Pantell, Proc. IRE, 47, 1146 (1959).

5. J.L. Hirshfield and J.M. Wachtel, Phys. Rev. Lett. 12, 533 (1964).

6. G. Bekefi, Jay L. Hirshfield and Sanborn C. Brown, Phys, Rev. 122, 1037 (1961).

7. J. L. Hirshfield, I.B. Bernstein and J.M. Wachtel, J. Quantum Electronics, Vol. QE-1, 237 (1965).

8. A.V. Gaponov, M. I. Petelin, and V. K. Yulpatov, Radiophys. Quantum Electron, 10, No. 9-10, 794-813 (1967).

9. A. V. Gaponov, and Y.K. Yulpatov, Radio Eng. Electron. Phys. 12, No. 4, 582-586 (1967).

10. G.N. Rapoport, A. K. Nemak, and V.A. Zhurakhovskiy, Radio Eng. Electron, Phys. 12, No. 4, 587-595 (1967).

11. Matthew Borenstein and Willis E. Lamb, Jr. Phys. Rev. A. 5, 1298 (1972).

12. V.L. Bratman, M.A. Moiseev, M.I.Petelin and R.E. Erm, Radiophys. Quantum Electron. 16, 474 (1973).

13. V.L. Bratman and A.E. Tokavev, Radiophys Quantum Electron. **17**, No. 8, 932-935 (1974).

14. P. Sprangle and Wallace M. Manheimer Phys. of Fluids, **18**, 224 (1975).

15. Edward Ott and Wallace M. Manheimer, IEEE Trans on Plasma Sci. Vol. PS-3, No. 1 (1975).

16. P. Sprangle, J. Applied Phys. **47**, 2935 (1976).

17. P. Sprangle and A.T. Drobot, IEEE Trans. on Microwave Theory and Techniques Vol. MTT-25, No. 6, 528 (June 1977).

18. K.R. Chu, Phys. of Fluids **21**, (Dec. 1978).

19. Hwan-sup Uhm, R.C. Davidson and K.R. Chu, Phys of Fluids **21**, 1866 (1978).

20. R.L. Schriever and C.C. Johnson, Proc. IEEE **54**, 2029 (1966).

21. D.V. Kisel', G.S. Korablev, V.G. Navel'yev, M.I. Petelin and Sh. E. Tsimring, Radio Engineering and Electronic Physics, **19**, 95 (1974).

22. N.I. Zaytsev, T.B. Pankratova, M.I. Petelin, and V.A. Flyagin, Radio Eng. Electron, Phys **19**, 103-106 (1974).

23. M. Friedman, D.A. Hammer, W.M. Manheimer and P. Sprangle, Phys. Rev. Letters **31**, 752 (1973).

24. V.L. Granatstein, P. Sprangle, M. Herndon, R.K. Parker and S.P. Schlesinger, Journal of Applied Physics **46**, 3800 (1975).

25. V.L. Granatstein, M. Herndon, P. Sprangle, Y. Carmel and J.A. Nation, Plasma Physics 17, 23 (1975).

26. V.L. Granatstein, P. Sprangle, M. Herndon and R.K. Parker, Journal of Applied Physics 46, 2021 (1975).

27. Jory, H., S. Hegji, J. Shively, and R. Symons, *Microwave J.* 21, 30 (1978).

28. V.A. Flyagin, A.V.Gaponov, M.I. Petelin and V.K. Yulpatov, IEEE Trans. Macrowave Theory Tech. MTT-25, 514 (1977).

29. J.L. Hirshfield and V.L Granatstein, IEEE Trans. Microwave Theory Tech. 25, 522 (1977).

30. A.A. Andronov, V.A. Flyagin, A.V. Gaponov, A.L. Gol'denberg, M.I. Petelin, V.G. Usov, and V.K. Yulpatov, report for Submillimeter Waves, Institute of Applied Physics, Gorky Academy of Sciences of the USSR (1978).

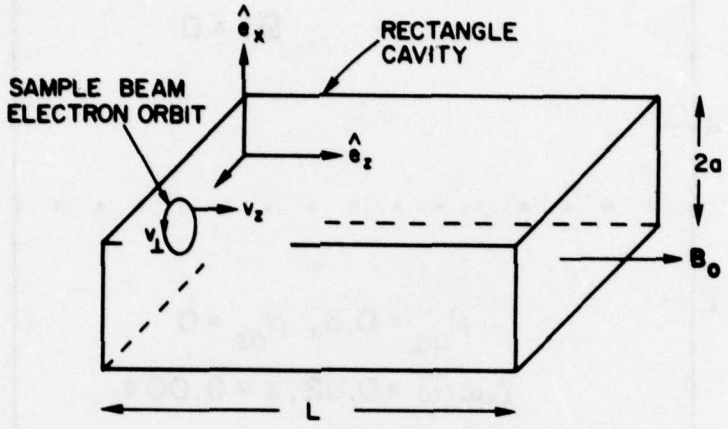

Fig. 1 — Model of the electron cyclotron maser cavity oscillator

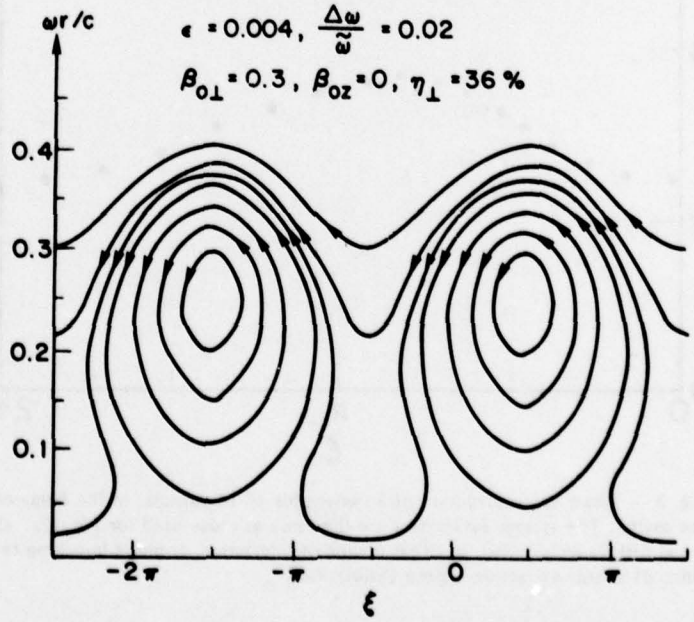

Fig. 2 — Typical phase space curves of the constant of motion $C(r, \xi)$

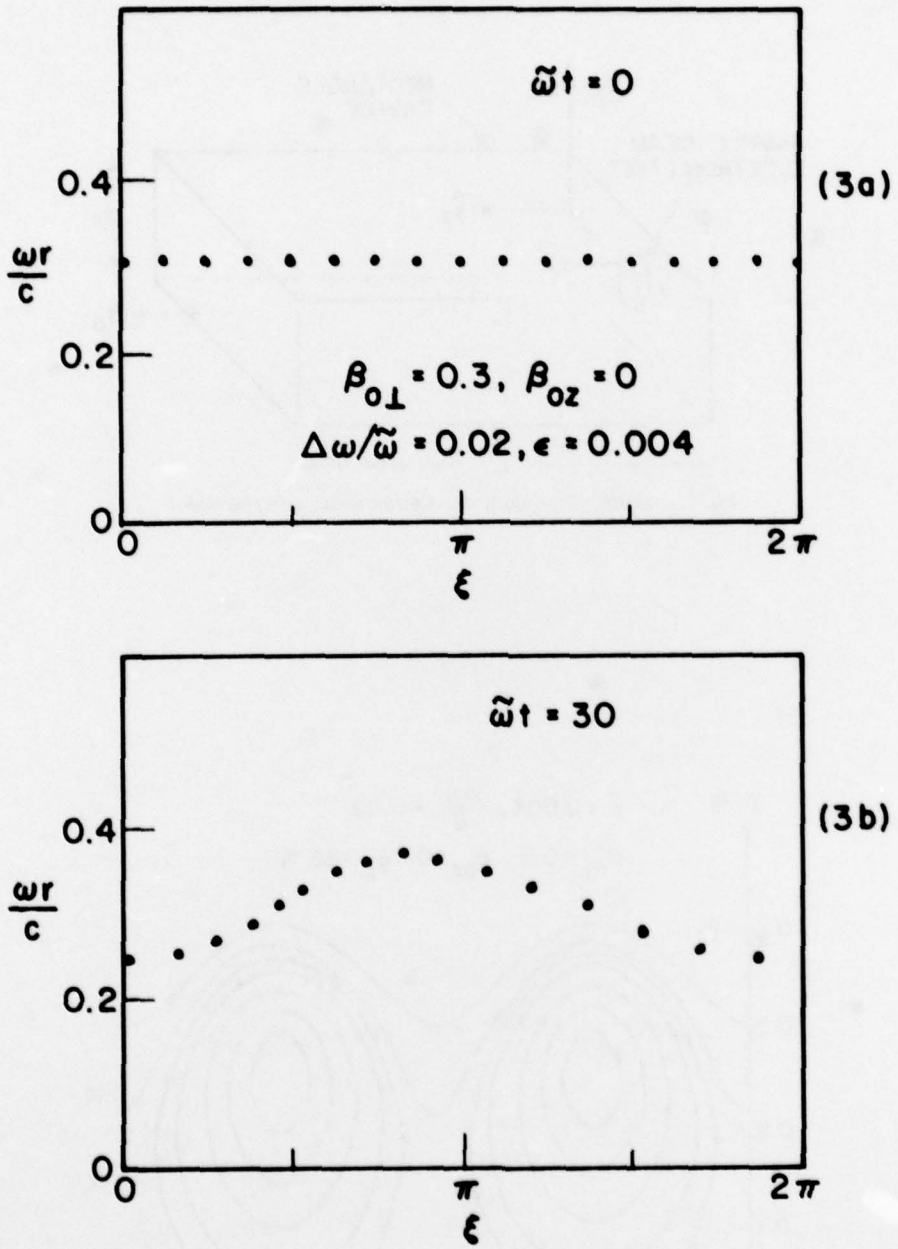

Fig. 3 — Phase space evolution of an ensemble of 16 particles in the fields of the cavity. The system parameters are the same as those used for Fig. (2). a) initial particle distribution. b) linear regime of interaction. c) phase bunching regime. d) energy extraction regime (Saturation).

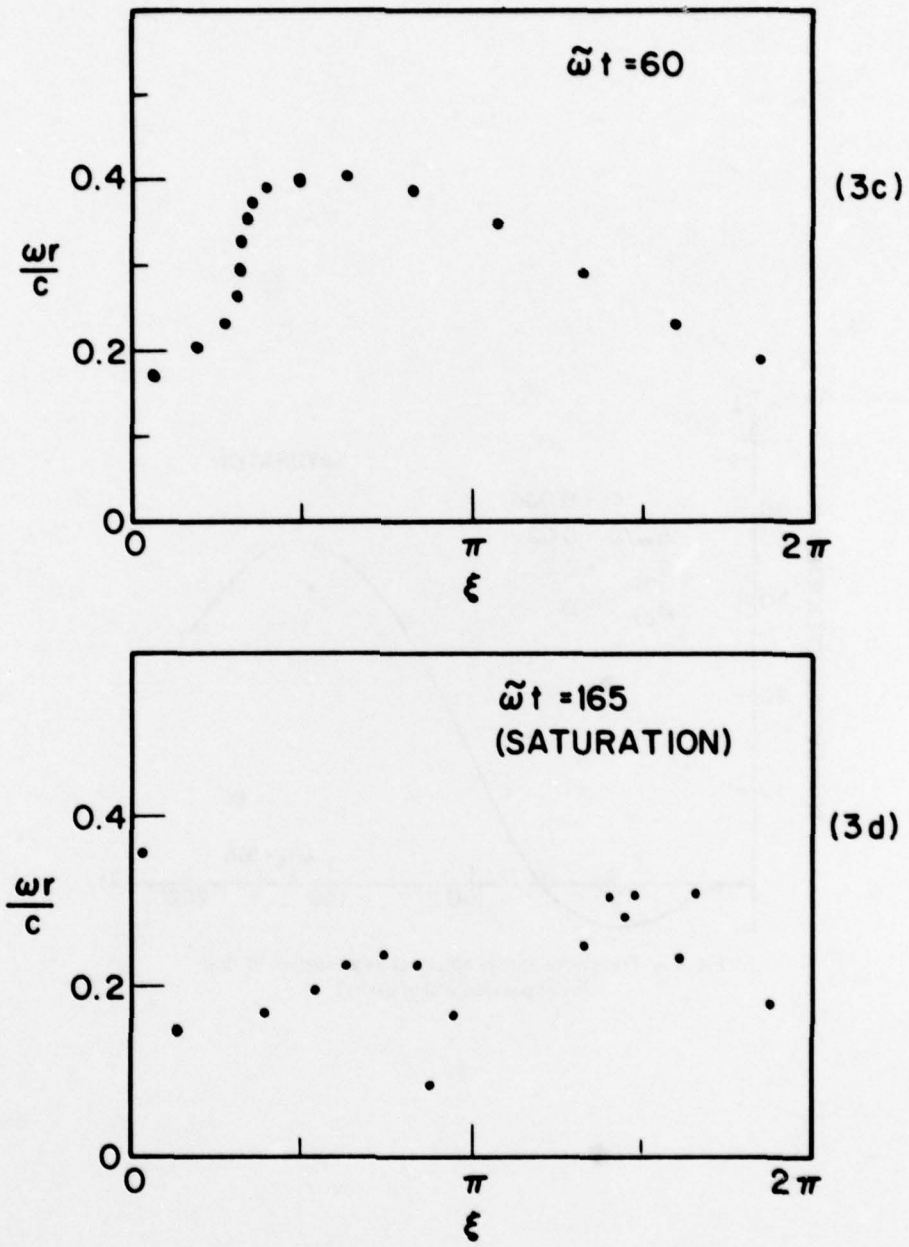

Fig. 3 (Continued) — Phase space evolution of an ensemble of 16 particles in the fields of the cavity. The system parameters are the same as those used for Fig. (2). a) initial particle distribution. b) linear regime of interaction. c) phase bunching regime. d) energy extraction regime (Saturation).

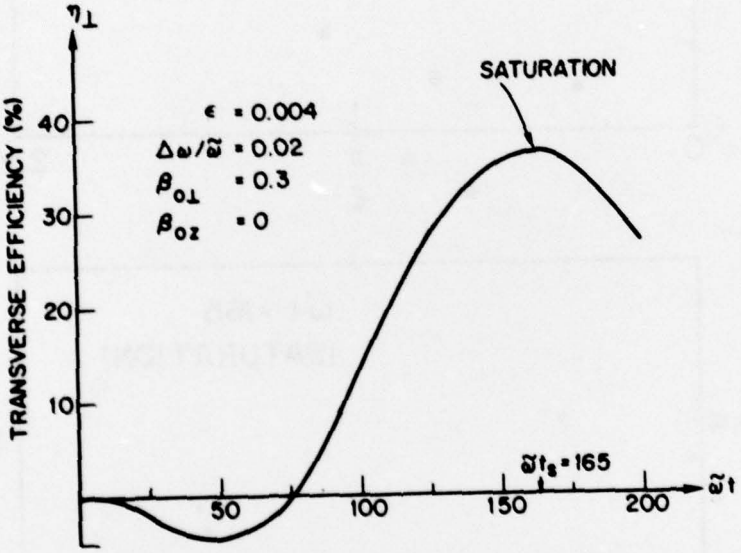

Fig. 4 — Transverse energy efficiency as a function of time (axial position within cavity)

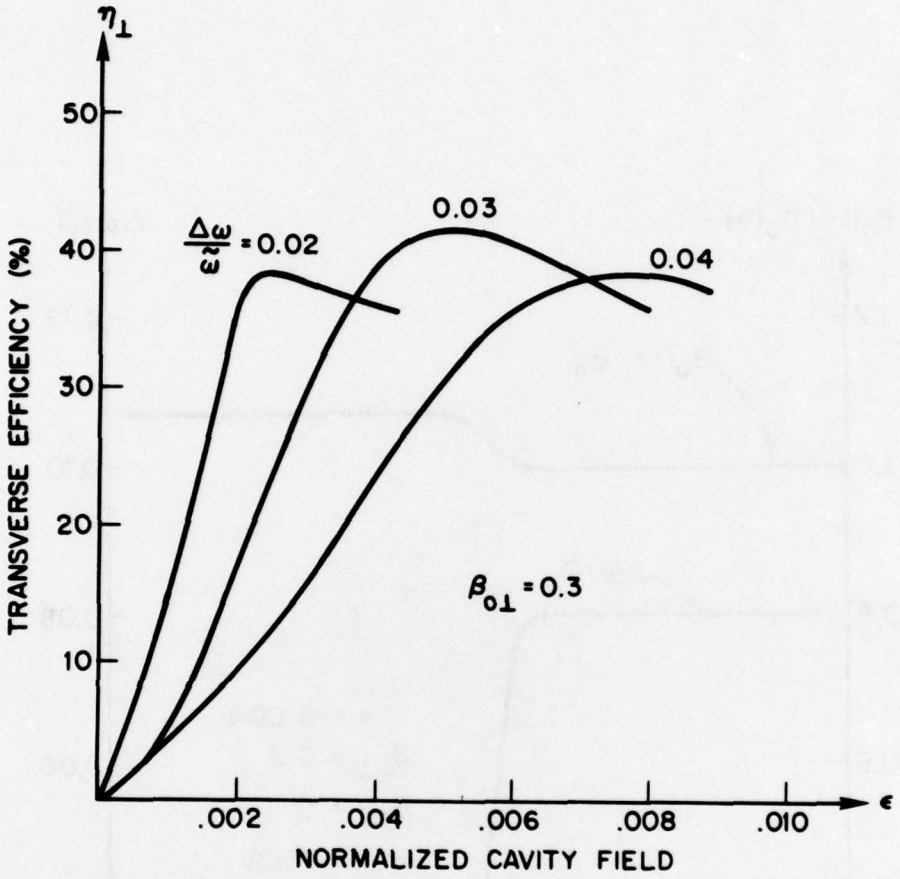

Fig. 5 — Saturation efficiences as a function of the normalized cavity field, ϵ, for various values of $\Delta\omega/\tilde{\omega}$. These results are for uniform B_o and K.

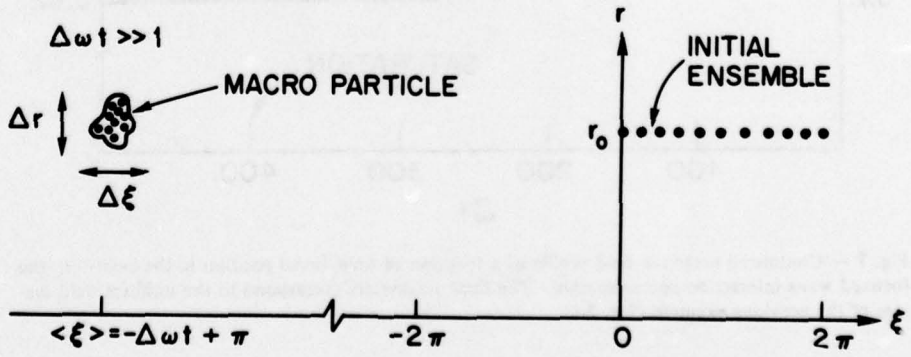

Fig. 6 — Schematic of phase space evolution illustrating the formation of a macro-particle when the bunching parameter, α, is much less than unity.

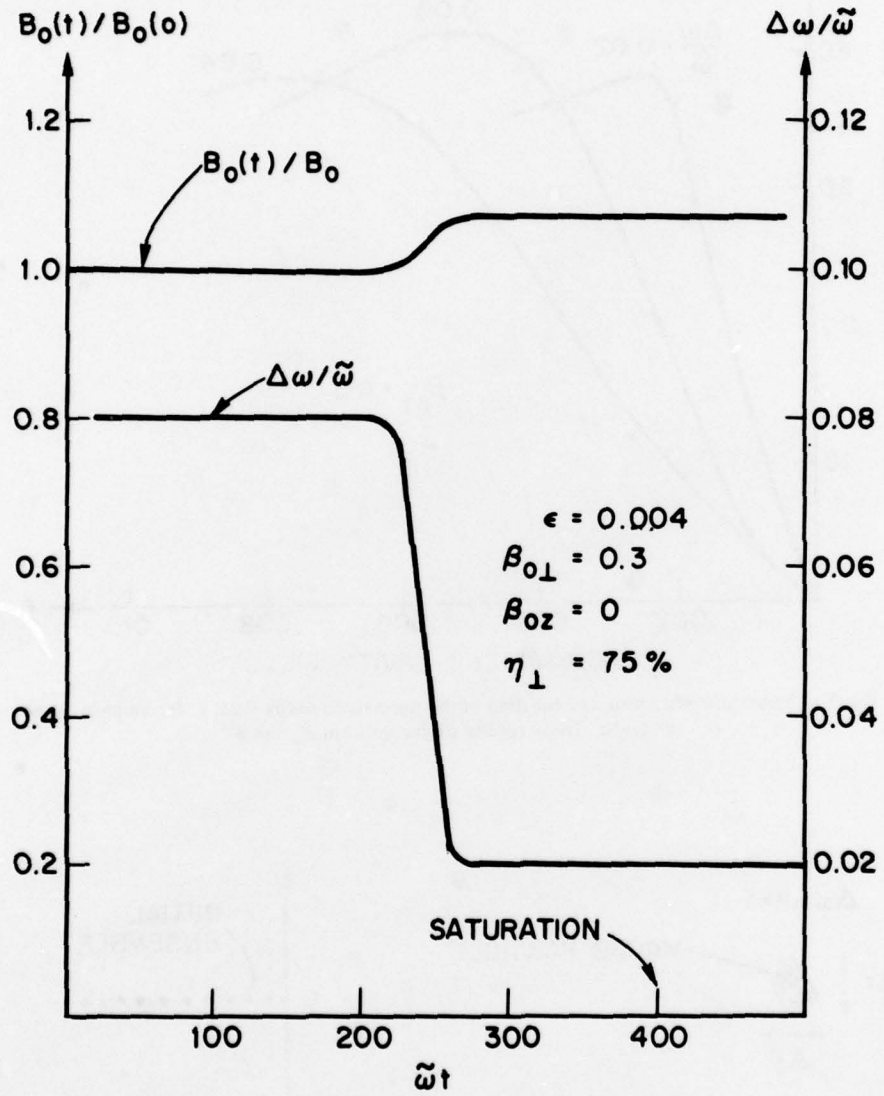

Fig. 7 — Contoured magnetic field profile as a function of time (axial position in the cavity) in the forward wave interaction approximation. The final parameters correspond to the uniform field system of the previous example (Fig. 2-4).

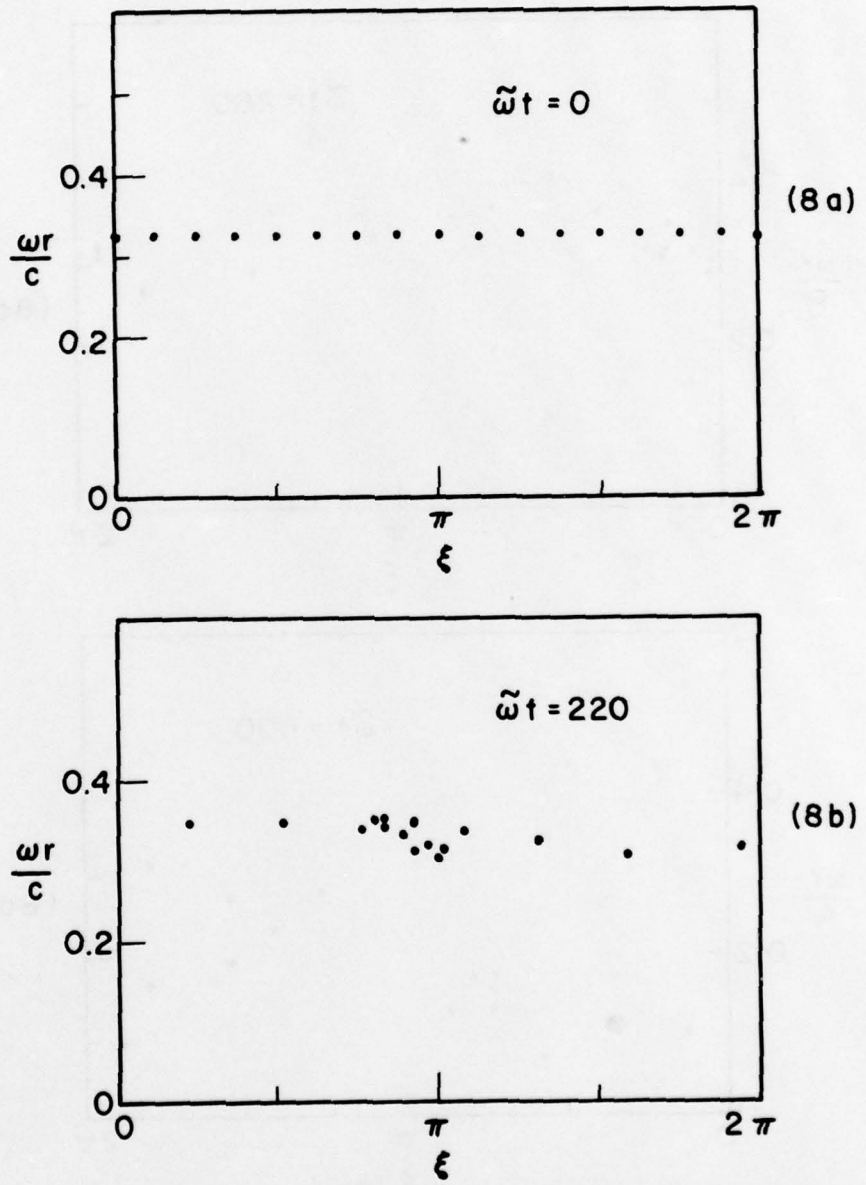

Fig. 8 — Phase space evolution for the field profile shown in Fig. 7: a) initial distribution of particles; b) formation of macro-particle just before entering contoured applied magnetic field region; c) the macro-particle after it leaves the contoured applied magnetic field region. d) particle distribution at saturation.

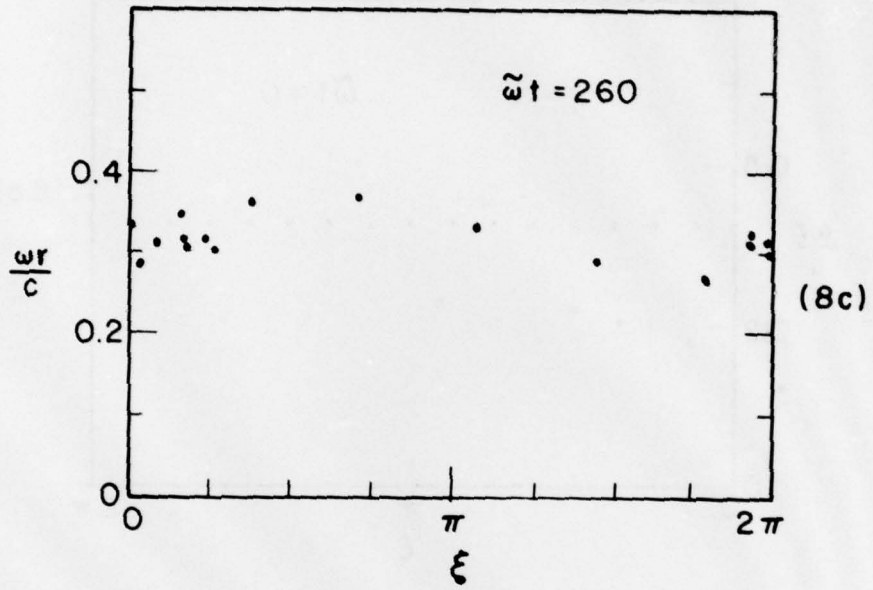

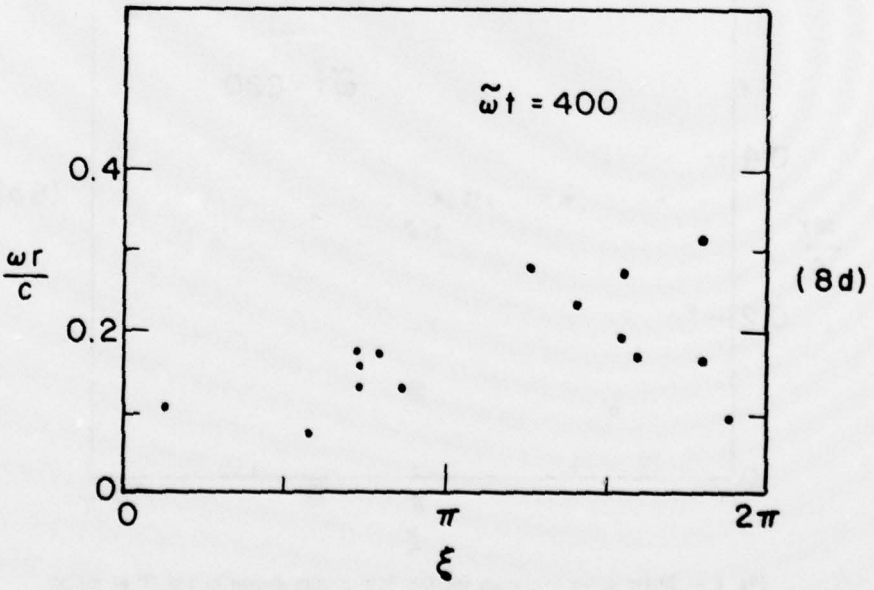

Fig. 8 (Continued) — Phase space evolution for the field profile shown in Fig. 7: a) initial distribution of particles; b) formation of macro-particle just before entering contoured applied magnetic field region; c) the macro-particle after it leaves the contoured applied magnetic field region; d) particle distribution at saturation.

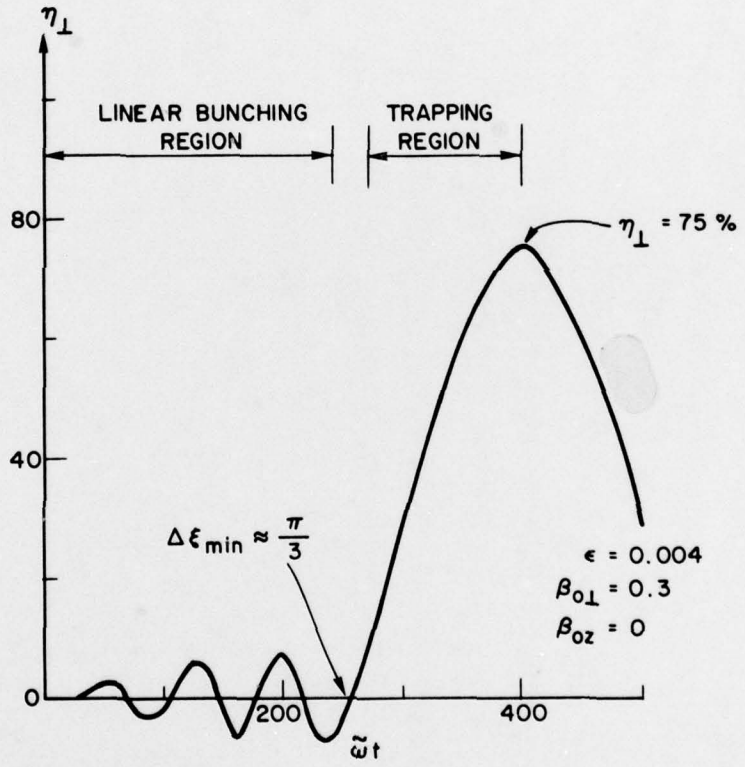

Fig. 9 — Transverse efficiency as a function of time (axial pos.tion in the cavity) for the system shown in Figs. (7) and (8).